Density-functional study of edge stress in graphene

Sukky Jun*
Department of Mechanical Engineering, University of Wyoming, Laramie, Wyoming 82071, USA
(Received 19 June 2008; published 22 August 2008)

The definition of edge stress is introduced in order to quantify the energy cost to deform a pre-existing edge in a two-dimensional crystal. Using density-functional *ab initio* calculations, edge stresses, as well as edge energies, are determined for the armchair and zigzag edges in graphene. It is found that both edges are under compression along the edge and the magnitude of compressive edge stress of armchair edge is larger than that of zigzag edge. In addition, hydrogen termination results in stress-free state for both edges. This excess edge quantity is expected to contribute to understanding various edge-related phenomena in graphene such as edge reconstructions and edge functionalizations.

DOI: 10.1103/PhysRevB.78.073405 PACS number(s): 61.46.−w, 61.48.De, 71.15.Mb

Graphene is a stable monolayer of hexagonal carbon lattice that has been isolated from bulk graphite by micromechanical exfoliation.[1] Intrigued by its unprecedented structural uniqueness as a strictly two-dimensional (2D) material, a great deal of research efforts have been made to unravel fundamental properties of graphene, such as chiral quantum Hall effects and zero-field conductivity.[2–6] In particular, more recent focuses have been on finite-sized graphene specimens in the form of ribbon or strip, in order to realize practical applications toward graphene-based nanoelectronics. For example, a field-effect transistor has successfully been demonstrated with graphene ribbons of less than 10 nm width.[7,8] Graphene nanoribbons reveal very unique properties such as special edge states,[9] half-metallicity,[10] lateral confinement of charge carriers, and band-gap opening.[11] A variety of edge functionalizations have also been explored to tailor their electronic, magnetic, and chemical properties.[12–16] These remarkable features of graphene nanoribbons are attributed to the existence of edge, the finite width, and the associated size effects. Therefore the understanding of the structural and electronic properties of graphene edge is of essential importance for the development of diverse nanoscale electronic, spintronic, and sensing devices.

Edge can be viewed as a line defect of a 2D crystalline monolayer. This notion reminds us of the importance of planar defects (e.g., surfaces and interfaces) in three-dimensional (3D) crystals. It is thus natural to deduce an analogy between edge and surface. As surface energy and surface stress play a combined role in describing various phenomena of surface-dominant 3D crystalline material systems,[17,18] edge-related unique properties of 2D crystals can potentially be understood through edge energy and edge stress. For example, a recent study has attempted to link edge energy to planar edge reconstructions in graphene nanoribbons.[19] However, to the best of the author's knowledge, there has not been any report on edge *stress* of a 2D crystal layer. In this work, we present the theoretical definition of edge stress, together with edge energy, by extending the idea of surface excess variables to this reduced-dimensional material system. Then, using density-functional *ab initio* calculations,[20,21] we determine the values of edge stress and edge energy for zigzag and armchair edges in graphene. In addition to free edges, hydrogen-terminated graphene edges are also considered to examine the effects of passivation on edge stress.

Let us recall surface energy and surface stress of a slab or a film of crystalline material. While surface energy is defined as the energy cost to create a surface, the energy cost to deform a surface is referred to as surface stress.[17,18,22–24] Analogy applies to a strictly 2D planar crystal layer having edges such as graphene nanoribbons. Edge energy γ is interpreted as the total excess energy possessed by all atoms close to the edge, normalized by the edge length L. This quantity defines the total work per unit length required to form a new edge. Edge stress f is defined as the unit reversible work involved in deforming a pre-existing edge. The relationship between edge energy and edge stress is represented by the Taylor expansion of edge energy under elastic strain limit (i.e., $\epsilon \ll 1$) as

$$\gamma(\epsilon) = \gamma_0 + f\epsilon, \tag{1}$$

where γ_0 is the edge energy when the edge is unstrained.

Following the Shuttleworth's representation of two reversible processes in creating and straining surfaces,[17,23,24] the edge stress can similarly be written in terms of the derivative of edge energy with respect to strain as $f = \gamma + d\gamma/d\epsilon$. Because we only consider deforming a 2D planar crystalline sheet along a straight edge, the associated stress and strain are both scalar (either positive or negative). Subjected to strain, the number of atoms per unit length and the electronic density of a crystal edge do change, which is the origin of the difference between edge energy and edge stress, represented by the last term $d\gamma/d\epsilon$ in the above equation.

The edge energy is calculated from the total-energy difference between model systems with and without edge, and the edge stress is basically obtained by fitting the calculated edge-energy values upon different amounts of strain. Therefore, the total-energy calculation is the key ingredient in numerically determining edge energy and edge stress alike. In what follows, the computational procedure employed in this work is described.

Ab initio total-energy calculations were performed using the program SIESTA (Ref. 25) that implements the pseudopotential approximation and the basis set of numerical atomic orbitals[26–29] into the framework of density-functional theory.[20,21] The norm-conserving nonlocal Troullier-Martins

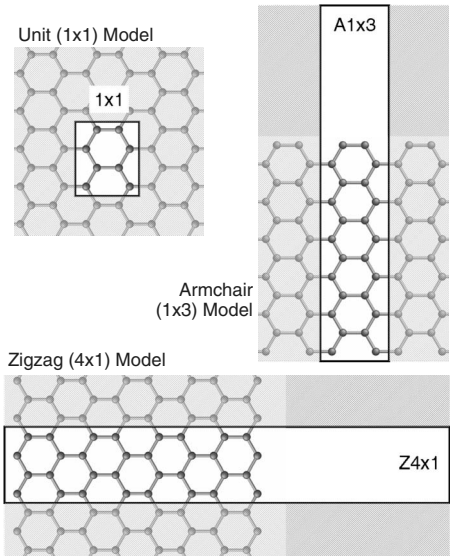

FIG. 1. Periodic supercells for graphene nanoribbons, such as zigzag (4×1) and armchair (1×3) models, are generated based on the unit (1×1) model. The longer sides of the vacuum area are kept 10 Å or larger. Shaded areas are shown for illustration only.

pseudopotential,[30] factorized in the Kleinman-Bylander separable form,[31] was employed with the core radius of 1.25 bohr for carbon atom. We employed local-density approximation (LDA) by using the Ceperley-Alder exchange-correlation functional[32] as parameterized by Perdew and Zunger.[33] A basis set of double-ζ plus polarization functions was used for the valence electrons of carbon atom with the energy shift parameter of 0.02 Ry.[25,34] An energy cutoff of 100 Ry was set for the real-space integrations. The relaxed atomic positions were obtained by the conjugate gradient optimization until the forces on each atom were smaller than 0.04 eV/Å. After relaxation with fully periodic boundary conditions, we obtained a graphene lattice constant 2.46 Å. It has been reported that the calculations of binding energy and elastic constants of graphene, with the above options, agree well with plane-wave calculations and experiment.[35] The method has also resulted in the band structure of graphite that is in good agreement with plane-wave pseudopotential calculations.[36]

Flat nanoribbon models were generated for the computation of edge energy and edge stress in graphene. We placed a graphene layer in a periodic 3D slablike supercell. The out-of-plane thickness of the supercell (i.e., the direction perpendicular to a flat graphene) was always set to be 10 Å which is sufficient to avoid the interaction between graphene layers caused by the periodicity. Edge energy is uniquely determined once an edge is identified. So is edge stress within the elastic range of strain. It implies that both excess variables are independent of the width of nanoribbon. To verify this, we considered several in-plane sizes with different ribbon widths, based upon the 8-atom unit model $(L_{x0}\times L_{y0})$, as depicted in Fig. 1. For example, the supercell of $Z4\times1$ zigzag edge model has a side length of $4L_{x0}+L_{\mathrm{vac}}$, four times greater than the unit length plus in-plane vacuum zone, in the direction perpendicular to the zigzag edge, while the other side has the same length L_{y0} as the unit model. The vacuum

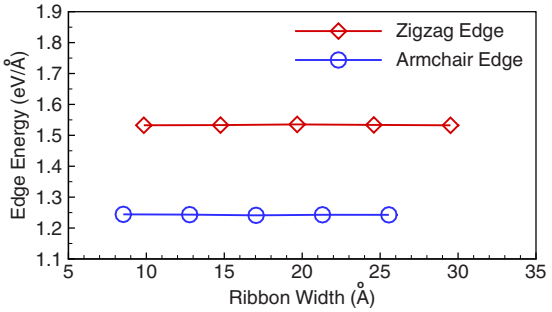

FIG. 2. (Color online) Calculated edge energies with respect to the width of graphene nanoribbon.

zone $(L_{\mathrm{vac}}\times L_{y0})$, with $L_{\mathrm{vac}}=10$ Å, was introduced in order to create two free edges and avoid the interaction between them. This modeling allows fully periodic boundary conditions on all six faces of the simulation box. Similar procedure was performed to build armchair edge models (e.g., $A1\times3$ as illustrated in Fig. 1). In this study, total 10 models of $Z2\times1$ up to $Z6\times1$ and $A1\times2$ up to $A1\times6$ were considered.

As mentioned above, edge energy is calculated from the total-energy difference between a graphene nanoribbon modeled as above (with the in-plane vacuum area) and a perfect graphene without edge (i.e., no vacuum area). However, special attention has to be paid because it has been reported that *ab initio* total-energy calculations of surface energy diverge with increasing slab thickness if there are numerical differences (e.g., k-point sampling) between the calculations for bulk and slab.[37] A recent study[38] has shown that the approach by Fiorentini and Methfessel[39] can effectively avoid such divergent behaviors of surface energy. For the calculation of edge energy, a similar equation is here introduced as

$$\gamma=\frac{1}{2L}(E^N_{\mathrm{ribbon}}-Ne_{\mathrm{graphene}}), \tag{2}$$

where E^N_{ribbon} denotes the total energy of the graphene nanoribbon having N carbon atoms in the supercell. L is the side length of the supercell along the edge, and e_{graphene} is the energy per atom in a perfect graphene without an edge. To determine e_{graphene}, we used the unit supercell model of eight carbon atoms (Fig. 1), and chose $10\times10\times1$ k-point mesh according to the Monkhorst-Pack scheme.[40] Total five E^N_{ribbon} values were calculated for zigzag edge, by employing $10\times10\times1$ k-point mesh for $Z2\times1$ $(N=16)$, $4\times10\times1$ for $Z3\times1$ $(N=24)$, $Z4\times1$ $(N=32)$, and $Z5\times1$ $(N=40)$, and $2\times10\times1$ for $Z6\times1$ $(N=48)$. Similar k-point meshes were selected for the armchair edge models such as $10\times10\times1$ for $A1\times2$, $10\times4\times1$ for $A1\times3$, and so on.

Results of edge energy with respect to the width of nanoribbon are shown in Fig. 2 that demonstrates nondivergent behaviors of edge energy. The average values are 1.533 eV/Å for zigzag edge and 1.243 eV/Å for armchair edge. All five ribbon widths agree within 0.2% for zigzag edge and within 0.3% for armchair edge, respectively. Armchair edge energy is therefore lower than zigzag edge energy by 0.290 eV/Å. This energetically favored armchair edge is

consistent with recent density-functional calculations,[19,41] and experiments by scanning tunneling microscopy.[42] Koskinen *et al.*[19] have calculated edge energies from the binding energy of graphene nanoribbons, which is equivalent to the above definition, Eq. (2). Using generalized-gradient approximation (GGA) (Ref. 43) and projector-augmented wave method,[44] they obtained 1.31 eV/Å for zigzag edge and 0.98 eV/Å for armchair edge. Both are commonly lower than the current LDA results. It is noted that similar trend has been found in the surface energy calculations for low Miller-index surfaces in 3D metallic slab where LDA resulted in larger surface energy than GGA.[38]

Armchair edge has C–C bonds that are parallel with the edge direction. After relaxation, the length of the armchair edge C–C bond was 1.24 Å which is shorter than the other parallel C–C bonds (~1.42 Å) away from the edge. It thus exhibits the strong pair of the *sp* hybridization and the higher charge density in the edge C–C bond than the interior bonds. This strong pairing heals the dangling-bond nature of the armchair edge C–C bond, resulting in lower edge energy than zigzag edge as discussed by Okada.[41] In contrast, no significant difference of C–C bond lengths between edge and interior was found in zigzag edge relaxation. This study by Okada[41] also implies that density-functional total-energy calculation can still be useful for reactive edges even though they involve multiple unpaired electrons.

Next, for the calculation of edge stress, a series of strains, from −0.6% up to +1.4% with the increment of 0.2%, were applied to three zigzag edge models ($Z2\times1$, $Z3\times1$, and $Z4\times1$) and three armchair edge models ($A1\times2$, $A1\times3$, and $A1\times4$). The same strains were also applied to the unit model given in Fig. 1. Then, using Eq. (2), we computed the edge energy for each strain state and each ribbon model. Therefore, 33 values of edge energy were collected, respectively, for zigzag and armchair edges (i.e., 11 strain states including zero strain, for 3 graphene models). Finally, these data were fitted to find the slope that is the edge stress itself, $f=(\gamma-\gamma_0)/\epsilon$, according to Eq. (1).

Results are shown in Fig. 3 where linear behaviors are well captured in the vicinity of $\epsilon=0$ (i.e., elastic limit). The values of edge stress are −2.248 eV/Å for zigzag edge and −2.640 eV/Å for armchair edge. Both are negative, which implies that both edges are under compression along the edge direction. In terms of magnitude, armchair edge stress is larger (i.e., under more compressive state) than zigzag edge stress by 0.392 eV/Å, which is in contrast to edge energies for which armchair edge has revealed a lower edge energy than zigzag edge by 0.290 eV/Å.

The negative edge stress means that an edge atom tends to push its neighboring edge atoms (i.e., increase the edge length) in order to lower its energy. This can be understood from the curve of total energy with respect to applied strain as shown in the inset of Fig. 3 where the total-energy values are in reference to that of unstrained edge. At zero strain, the curve has negative slope. The lowest total energy thus corresponds to a certain positive strain, that is, tension along the edge. An edge atom tries to push its neighboring edge atoms away in order to increase the edge length, reduce its energy, and reach a lower-energy state. In other words, at the zero strain, an edge atom is experiencing compressive edge stress.

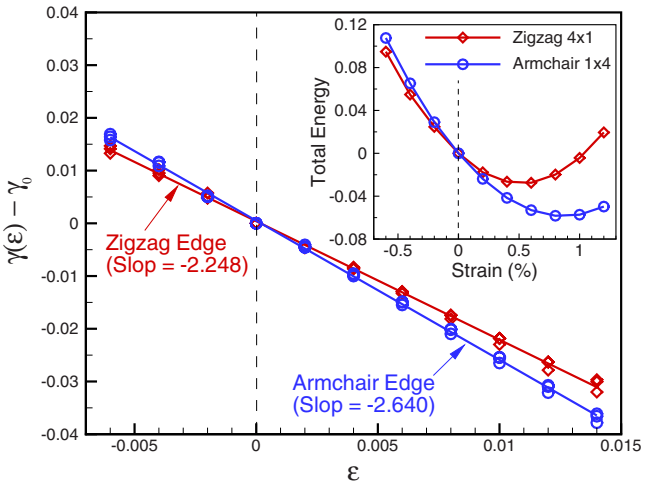

FIG. 3. (Color online) Excess edge energies (eV/Å) with respect to applied strains. The slope is edge stress (eV/Å). (Inset) Total energies of zigzag (4×1) and armchair (1×4) nanoribbon models with respect to applied strains.

Finally, we considered hydrogen-terminated edges in order to investigate the effect of hydrogen passivation on the reduction of edge stresses. In the above, edge stress were determined from the difference of edge energies between strained and unstrained systems. For the unstrained system, we used the unit model of perfect graphene without edge (Fig. 1). However, for hydrogen-terminated edges, we have to use another approach since we cannot directly compare the perfect graphene model with edged graphenes, due to the existence of hydrogen atoms. Therefore, for such edges, we employed a method based on the additive property of elastic strain energy that has successfully been used to investigate the adatom effects on surface stress of Cu surfaces (see Pao *et al.*[45] for details). Revising their method to suit the two-dimensional graphene layer, we obtained the edge stresses of 0.006 eV/Å for zigzag edge and −0.017 eV/Å for armchair edge. Both are negligible amounts of stress compared with the corresponding free edges. This indicates that hydrogen termination turns the compressive states of edge stress into almost stress-free ones.

In summary, we have defined edge stress as the energy cost to deform a pre-existing edge in an isolated two-dimensional crystalline monolayer. Using density-functional *ab initio* calculations, edge energy and edge stress have been determined for the armchair and zigzag edges in graphene. Both edges are under compression along the edge. While armchair edge energy is lower than zigzag edge energy, the magnitude of compressive edge stress of armchair edge is larger than that of zigzag edge. Furthermore, hydrogen terminations result in stress-free edges. These excess edge variables are expected to play a key role in examining various edge-related phenomena in graphene such as edge reconstructions and edge functionalizations.

This work was supported in part by a Faculty Grant-in-Aid program from the University of Wyoming. The author appreciates helpful discussion with Changwen Mi.

*sjun@uwyo.edu

[1] K. S. Novoselov, A. K. Geim, S. V. Morozov, D. Jiang, Y. Zhang, S. V. Dubonos, I. V. Grigorieva, and A. A. Firsov, Science **306**, 666 (2004).
[2] A. K. Geim and K. S. Novoselov, Nat. Mater. **6**, 183 (2007).
[3] K. S. Novoselov, A. K. Geim, S. V. Morozov, D. Jiang, M. I. Katsnelson, I. V. Grigorieva, S. V. Dubonos, and A. A. Firsov, Nature (London) **438**, 197 (2005).
[4] Y. Zhang, J. W. Tan, H. L. Stormer, and P. Kim, Nature (London) **438**, 201 (2005).
[5] J. R. Williams, L. DiCarlo, and C. M. Marcus, Science **317**, 638 (2007).
[6] D. A. Abanin and L. S. Levitov, Science **317**, 641 (2007).
[7] X. Li, X. Wang, L. Zhang, S. Lee, and H. Dai, Science **319**, 1229 (2008).
[8] X. Wang, Y. Ouyang, X. Li, H. Wang, J. Guo, and H. Dai, Phys. Rev. Lett. **100**, 206803 (2008).
[9] K. Nakada, M. Fujita, G. Dresselhaus, and M. S. Dresselhaus, Phys. Rev. B **54**, 17954 (1996).
[10] Y.-W. Son, M. L. Cohen, and S. G. Louie, Nature (London) **444**, 347 (2006).
[11] M. Y. Han, B. Özyilmaz, Y. Zhang, and P. Kim, Phys. Rev. Lett. **98**, 206805 (2007).
[12] Q. Yan, B. Huang, J. Yu, F. Zheng, J. Zang, J. Wu, B.-L. Gu, F. Liu, and W. Duan, Nano Lett. **7**, 1469 (2007).
[13] O. Hod, V. Barone, J. E. Peralta, and G. E. Scuseria, Nano Lett. **7**, 2295 (2007).
[14] Z. F. Wang, Q. Li, H. Zheng, H. Ren, H. Su, Q. W. Shi, and J. Chen, Phys. Rev. B **75**, 113406 (2007).
[15] D. Gunlycke, J. Li, J. W. Mintmire, and C. T. White, Appl. Phys. Lett. **91**, 112108 (2007).
[16] F. Cervantes-Sodi, G. Csányi, S. Piscanec, and A. C. Ferrari, Phys. Rev. B **77**, 165427 (2008).
[17] R. C. Cammarata, Prog. Surf. Sci. **46**, 1 (1994).
[18] H. Ibach, Surf. Sci. Rep. **29**, 195 (1997).
[19] P. Koskinen, S. Malola, and H. Häkkinen, arXiv:0802.2623 (unpublished).
[20] P. Hohenberg and W. Kohn, Phys. Rev. **136**, B864 (1964).
[21] W. Kohn and L. J. Sham, Phys. Rev. **140**, A1133 (1965).
[22] J. W. Gibbs, *The Collected Works of J. W. Gibbs* (Longmans, New York, 1928), Vol. 1, p. 315.
[23] R. Shuttleworth, Proc. Phys. Soc., London, Sect. A **63**, 444 (1950).
[24] J. W. Cahn and F. Larche, Acta Metall. **30**, 51 (1982).
[25] J. Soler, E. Artacho, J. D. Gale, A. García, J. Junquera, P. Ordejón, and D. Sánchez-Portal, J. Phys.: Condens. Matter **14**, 2745 (2002).
[26] P. Ordejón, Comput. Phys. Commun. **12**, 157 (1998); S. Goedecker, Rev. Mod. Phys. **71**, 1085 (1999).
[27] J. Kim, F. Mauri, and G. Galli, Phys. Rev. B **52**, 1640 (1995).
[28] P. Ordejón, D. A. Drabold, M. P. Grumbach, and R. M. Martin, Phys. Rev. B **48**, 14646 (1993).
[29] F. Mauri, G. Galli, and R. Car, Phys. Rev. B **47**, 9973 (1993).
[30] N. Troullier and J. L. Martins, Phys. Rev. B **43**, 1993 (1991).
[31] L. Kleinman and D. M. Bylander, Phys. Rev. Lett. **48**, 1425 (1982).
[32] D. M. Ceperley and B. J. Alder, Phys. Rev. Lett. **45**, 566 (1980).
[33] J. P. Perdew and A. Zunger, Phys. Rev. B **23**, 5048 (1981).
[34] E. Artacho, D. Sánchez-Portal, P. Ordejón, A. García, and J. M. Soler, Phys. Status Solidi B **215**, 809 (1999).
[35] S. Reich, C. Thomsen, and P. Ordejón, Phys. Rev. B **65**, 153407 (2002).
[36] S. Reich, J. Maultzsch, C. Thomsen, and P. Ordejón, Phys. Rev. B **66**, 035412 (2002), and references therein.
[37] J. C. Boettger, Phys. Rev. B **49**, 16798 (1994).
[38] N. E. Singh-Miller and N. Marzari, arXiv:0801.1077 (unpublished).
[39] V. Fiorentini and M. Methfessel, J. Phys.: Condens. Matter **8**, 6525 (1996).
[40] H. J. Monkhorst and J. D. Pack, Phys. Rev. B **13**, 5188 (1976).
[41] S. Okada, Phys. Rev. B **77**, 041408(R) (2008).
[42] Y. Kobayashi, K.-I. Fukui, T. Enoki, and K. Kusakabe, Phys. Rev. B **73**, 125415 (2006).
[43] J. P. Perdew, K. Burke, and M. Ernzerhof, Phys. Rev. Lett. **77**, 3865 (1996).
[44] P. E. Blöchl, Phys. Rev. B **50**, 17953 (1994).
[45] C.-W. Pao, D. J. Srolovitz, and C. V. Thompson, Phys. Rev. B **74**, 155437 (2006).